

Pressure-induced phonon freezing in the $\text{Zn}_{1-x}\text{Be}_x\text{Se}$ alloy: A study via the percolation modelGopal K. Pradhan,¹ Chandrabhas Narayana,¹ O. Pagès,^{2,*} A. Breidi,² J. Souhabi,² A. V. Postnikov,² S. K. Deb,³ F. Firszt,⁴ W. Paszkowicz,⁵ A. Shukla,⁶ and F. El Haj Hassan⁷¹*Light Scattering Laboratory, Chemistry and Physics of Materials Unit, Jawaharlal Nehru Centre for Advanced Scientific Research (JNCASR), Jakkur P.O., Bangalore 560064, India*²*Laboratoire de Physique des Milieux Denses–IJB, Université Paul Verlaine, Metz 57078, France*³*Indus Synchrotron Utilization Division, RRCAT, Indore 452013, India*⁴*Institute of Physics, N. Copernicus University, 87-100 Toruń, Poland*⁵*Institute of Physics, Polish Academy of Sciences, 02-668 Warsaw, Poland*⁶*Institut de Minéralogie et de Physique des Milieux Condensés–CNRS-UMR7590,**Université Pierre et Marie Curie–Paris 6, 140 rue de Lourmel, Paris F-75015, France*⁷*Laboratoire de Physique des Matériaux, Université Libanaise, El Hadath, Beyrouth, Lebanon*

(Received 26 October 2009; revised manuscript received 18 December 2009; published 11 March 2010)

We use the 1-bond \rightarrow 2-phonon percolation doublet of zinc-blende alloys as a “mesoscope” for an unusual insight into their phonon mode behavior under pressure. We focus on (Zn,Be)Se and show by Raman scattering that the application of pressure disables an anharmonic coupling between the nominal Zn-Se zone-center TO mode and disorder-activated two-phonon zone-edge continua. This reveals an unexpectedly clear percolation-type fine structure of the Zn-Se TO mode, the latter fine structure being unaffected by pressure. In contrast, the original Be-Se doublet at ambient pressure, of the stretching-bending type, turns into a pure-bending singlet at the approach of the high-pressure ZnSe-like rocksalt phase, an unnatural one for the Be-Se bonds. The “freezing” of the Be-Se stretching mode is discussed within the scope of the percolation model (mesoscopic scale), supported by *ab initio* insight into the pressure dependence of vibrational properties of the ultimate percolation-type Be-impurity motif (microscopic scale). Similar *ab initio* calculations are performed with (Ga,As)P, for reference purpose.

DOI: [10.1103/PhysRevB.81.115207](https://doi.org/10.1103/PhysRevB.81.115207)

PACS number(s): 63.50.–x, 81.40.Vw

I. INTRODUCTION

Recently, a unified understanding of the phonon mode behavior of usual $A_{1-x}B_xC$ semiconductor alloys with fourfold-coordinated cubic zinc-blende (ZB) structure, as conveniently observed at the laboratory scale by using optical spectroscopies (such as Raman scattering and infrared absorption), could be achieved within the so-called percolation model developed by one of us (O.P.). In this model a random alloy is viewed as a composite of the AC- and BC-like regions, where A-C and B-C bonds are highly self-connected, respectively, each region providing one phonon per bond (1-bond \rightarrow 2-mode).¹ This reveals that phonons give a natural insight into the alloy disorder at the unusual mesoscopic scale. We introduced a terminology that the percolation doublet (with splitting denoted by Δ) acts as a “mesoscope” into the alloy disorder. In principle, the change in frequency and intensity of each 1-bond \rightarrow 2-mode mesoscope (AC- and BC-like) may be studied under the influence of any stimulus. This opens the way for a basic understanding beyond that given by the usual 1-bond \rightarrow 1-mode “macroscope” of Chang and Mitra,² based on a description of an alloy as a uniform continuum according to the virtual-crystal approximation (VCA).

In this work, we explore what the mesoscope may say about the phonon behavior of semiconductor alloys under pressure. The aim is to decide whether the AB- and AC-like regions are affected in the same way by hydrostatic pressure or whether one region behaves in a specific manner.

The most suitable alloy to address such issue is $\text{Zn}_{1-x}\text{Be}_x\text{Se}$. While ZnSe adopts the usual sixfold-

coordinated cubic NaCl [metallic rocksalt (RS)] phase under pressure, BeSe is one of the few exceptional systems that transforms to the sixfold-coordinated hexagonal NiAs phase.^{3,4} Furthermore, the transition pressure is much higher for BeSe (~ 56 GPa) than for ZnSe (~ 13 GPa). Besides, Luo *et al.*⁴ observed that the volume collapse for BeSe ($\sim 11\%$) is small as compared with ZnSe ($\sim 17\%$); in fact the smallest ever achieved at a first-order fourfold-to-sixfold phase transition.⁴ They advanced an idea that due to the small size of the Be cations there exists a strong Pauling repulsive interaction between the large-size Se anions, which prevents drastic volume reduction.

An interesting question then is what happens to the Be-Se bonds of ZnBeSe crystals with moderate Be content when the ZnSe-like medium begins its natural ZB \rightarrow RS transition, an unnatural one for the Be-Se bond? This we investigate by taking advantage of the well-resolved Be-Se mesoscope ($\Delta \sim 40$ cm^{-1}). We perform Raman measurements at increasing pressure up to the ZB \rightarrow RS transition using a series of alloys with moderate Be content that allows to cover all possible topologies of the BeSe-like region as determined by two critical x values. The first is the Be-Se bond percolation threshold ($x_{\text{Be}}=0.19$), at which limit the spatial organization of the BeSe-like region turns from a dispersion of finite-size clusters ($x < x_{\text{Be}}$) into a pseudoinfinite treelike continuum ($x > x_{\text{Be}}$), and the second is $x=0.5$, beyond which limit the latter continuum becomes dominant over the coexisting ZnSe-like one.⁵ We then attempt to achieve consistent understanding of the observed effects at both the mesoscopic (percolation scheme) and microscopic (*ab initio* calculations) scales.

The manuscript is organized as follows. In Sec. II we give the experimental details and present briefly the *ab initio* methods. The experimental results are reported in Sec. III. The specific behaviors in the Zn-Se and Be-Se spectral ranges are separately discussed in Secs. III A and III B, respectively. In each spectral range the discussion is supported by *ab initio* insight into the pressure dependence of the transverse optical (TO) density of states at the Brillouin zone center (ZC TO-DOS, directly compared with Raman spectra) of a prototype impurity motif. In Sec. III B the *ab initio* calculations are extended to the Ga-P bond of GaAsP, for reference purpose. Conclusions are summarized in Sec. IV.

II. EXPERIMENTAL DETAILS AND *AB INITIO* METHODS

Zn_{1-x}Be_xSe single crystals with x values of 0.11, 0.16, 0.24, and 0.55 (the largest achievable limit so far), measured by x-ray diffraction, were grown by the Bridgman method. For each sample a (111)-oriented cleaved piece was polished to a ~ 25 - μm -thick platelet and placed together with ruby chips into a 200- μm -thick stainless-steel gasket (preindented to 65 μm) inserted between the diamonds of a Mao/Bell-type diamond-anvil cell. Methanol/ethanol/water (16:3:1) was used as pressure transmitting medium, the pressure being determined via the ruby fluorescence linear scale. The pressure environment is assured to be hydrostatic until ~ 14 GPa, beyond which it can be treated quasihydrostatic until ~ 30 GPa. Unpolarized Raman spectra were recorded in backscattering geometry on the (111) crystal face with the nonresonant 532.0 nm excitation. In such geometry both the TO and longitudinal optical (LO) modes are Raman active. We recall that these modes consist of out-of-phase vibrations of the quasirigid anion (Se) and cation (Zn,Be) sublattices, either perpendicular to (TO) or along (LO) the direction of propagation.

Ab initio ZC TO-DOS calculations were done with the SIESTA code.⁶ We used 64 atom supercells containing the “ultimate” percolation motif (referred to as the 2-imp. motif), i.e., a pair of next-nearest-neighbor impurities (say *A*) immersed in the environment of the other species (*BC*-like). Both the ZnBeSe and GaAsP alloys were considered (the latter for reference purpose), using the basis of pseudopotentials set up in Refs 1 and 7, respectively. After performing the full relaxation of lattice parameters and atomic positions within each supercell, the dynamical matrix was constructed by probing small individual displacements of atom from their equilibrium positions and collecting the forces induced on all sites. The diagonalization of the dynamical matrix yielded the frequencies of TO phonons and the corresponding eigenvectors. A subsequent projection of eigenvectors onto the uniform translation pattern of each species throughout the crystal, as explained in Ref. 7, permits to single out the vibrations of genuinely zone-center character. The correspondingly weighted (and artificially broadened) spectrum of discrete vibration frequencies can then be compared with the TO Raman spectrum. It should be noted that the matrix elements of Raman scattering were not taken into account in the calculation, so that the relative magnitudes of different peaks

do not always mimic those in the experiment.

III. RESULTS AND DISCUSSION

Before entering the body of the discussion we briefly specify the general context of the study, as derived from preliminary x-ray diffraction measurements performed over the investigated pressure domain (not shown). The basic trend is that the ZB \rightarrow RS transition is regularly shifted to higher pressure when the incorporation of Be increases. This is due to the reinforcement of the highly ionic (soft) ZnSe lattice by the strongly covalent (stiff) Be-Se bonds. Besides, the x-ray diffraction data indicate that the ZB \rightarrow RS transition is very sharp, and that the crystal adopts the RS structure as a whole. Indeed no signal due to any residual ZB phase could be detected beyond the transition pressure.⁸

In the discussion of the Raman data we focus on TO modes, because such purely mechanical vibrations do not couple, and, as such, give reliable insight into the individual percolation-type oscillators present in the crystal.¹ In labeling of the TO modes the subscript and superscript refer to the bond species and to the host region, respectively. In contrast, in zinc-blende alloys the close LO modes of each percolation doublet couple via the accompanying macroscopic polarization due to the ionicity of the bonds, which results in a unique LO mode.¹ The percolation doublet thus disappears in the LO symmetry, and with it the mesoscopic insight.

For the presentation and discussion of the data we focus on the intermediate x value ($x=0.24$), which corresponds to well-resolved Zn-Se and Be-Se Raman signals, but the effects are general. Representative pressure-dependent Raman spectra are shown in Fig. 1. The frequency versus pressure variations of the main features are shown in the inset. A 2TO+1LO percolation signal shows up clearly in the Be-Se spectral range (~ 550 cm^{-1}). In the Zn-Se spectral range (~ 225 cm^{-1}), the assignment is more difficult due to the existence of several modes. Although a preliminary 1TO+1LO assignment was earlier proposed by some of us, the current high-pressure data lead to a more refined one (see below).

With increasing pressure the intensity of the LO modes decreases, a well-known effect of the progressive metallization of the sample resulting in the ZB \rightarrow RS transition. The total LO extinction occurs at ~ 23 GPa, coinciding with the actual ZB \rightarrow RS transition observed by x-ray diffraction (not shown).⁸ More fascinating effects relate to TO modes as marked by capitals, i.e., (A) the splitting of the lower Zn-Se branch, (B) the transient emergence of a weak mode in between two main Zn-Se branches, and (C) the convergence of the lower Be-Se TO branch onto the upper one.

A. Zn-Se spectral range

First, we focus on the Zn-Se spectral range. A natural reference is the pressure dependence of the Raman frequencies in pure ZnSe, as reproduced in Fig. 2 (symbols, digitalized from Ref. 9). The two sub-branches that proceed from the “nominal” TO mode at ~ 2 (refer to the dotted arrow in Fig. 2) and ~ 7 GPa are usually interpreted as TO modes due

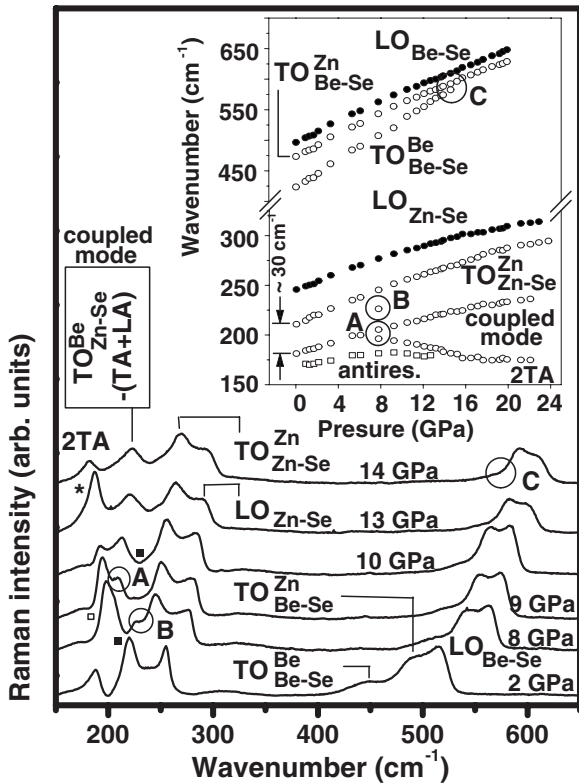


FIG. 1. Pressure dependent Raman spectra of $Zn_{0.76}Be_{0.24}Se$. The frequency versus pressure variations of the main features are shown in the inset. There, the plain and open circles refer to the LO and TO modes, respectively. Remarkable trends (A,B,C) are marked by circles. The antiresonances (squares) and the strong peak (star) are characteristic of anharmonic coupling.

to intermediate phases in between the ZB and RS ones. However, no such phases could be identified in ZnSe yet, neither experimentally nor by *ab initio* calculations.¹⁰ Our view is rather that the entire ZnSe spectrum results from an anharmonic decay of the discrete (zone center) TO into at least two two-phonon continua (corresponding to the two sub-branches), or, in general, into a variety of such. Characteristic features are discussed below.

In such decay process, conservations of the momentum and energy impose equal and opposite wave vectors of the two phonons (because Raman scattering operates at the Brillouin-zone center), and quasisonance of the discrete TO and two-phonon continua. Referring to the phonon DOS of pure ZnSe,¹¹ the likely continua are the 2TA and TA+LA originating from the transverse (TA) and longitudinal (LA) acoustical branches at the K and L Brillouin-zone edges, respectively. Under pressure, the discrete TO and two-phonon continua decouple because different pressure dependencies lead to a departure from resonance conditions. In ZnSe, the zone-edge TA phonons “soften” under pressure, while the zone-center TO and zone-edge LA “harden” fast.¹² The TA trend reinforces in the 2TA continuum, while it is more or less compensated by the opposite LA trend in the TA+LA continuum. We thus reassign the two branches that proceed from the “nominal” TO at ~ 2 and ~ 7 GPa in pure ZnSe, with large-negative and small-positive pressure coef-

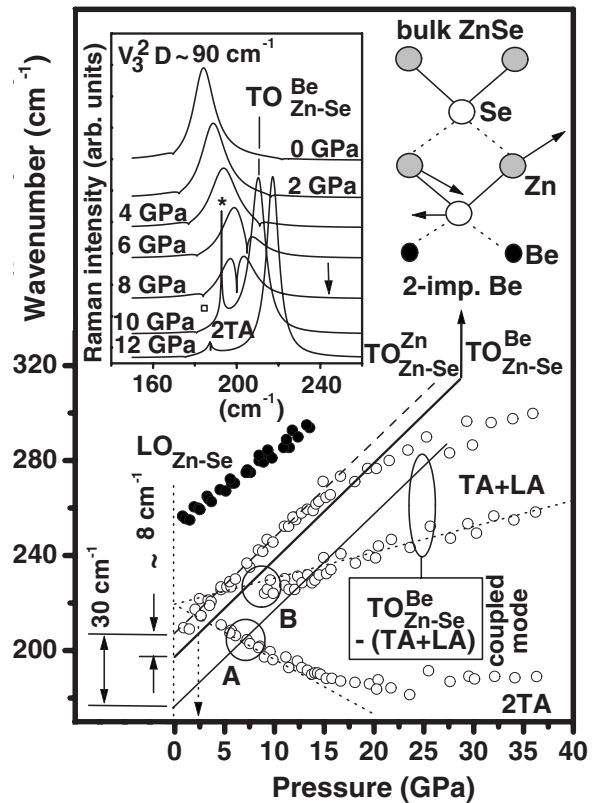


FIG. 2. Schematic explanation of the features A and B (circles) by referring to pure ZnSe [plain (LO) and open (TO) symbols, digitalized from Ref. 9]. In the alloy the weak TO_{Zn-Se}^{Be} mode (thick line—in the corresponding vibration pattern the dotted and plain lines indicate perpendicular planes) appears on top of the strong TO_{Zn-Se}^{Zn} one (pure-ZnSe-like, dashed line). The natural splitting of $\sim 8 \text{ cm}^{-1}$ is magnified to $\sim 30 \text{ cm}^{-1}$ by an anharmonic coupling that downshifts the weak mode from the thick line to the thin one. The line shapes of the weak mode over its decoupling process are shown in the inset. The star and squares mark features characteristic of anharmonic coupling, as in Fig. 1. At 8 GPa an arrow marks the position of the harmonic mode, for reference purpose.

ficients, as the 2TA and TA+LA continua, respectively.

The A and B features in Fig. 1 can then be simply explained by considering that in the alloy a weak extra TO appears and substitutes for the strong (pure-ZnSe-like) TO for the anharmonic decay into the 2TA continuum. The principle is outlined in Fig. 2. The weak TO is represented by a thin line downshifted from the strong TO (dashed line) by $\sim 30 \text{ cm}^{-1}$. With this, the 2TA-decoupling is delayed from ~ 2 GPa in pure ZnSe (from the strong TO, see the dotted arrow) to ~ 7 GPa in the alloy (from the weak TO), in reference to A, while B at ~ 7 GPa is due to transient appearance of the TA+LA continuum just after decoupling from the strong TO and before recoupling with the weak TO (see the oval). In fact the coupling-related antiresonance in between the two TO (solid squares in Fig. 1) disappears in this intermediate decoupling regime (see the spectrum at ~ 9 GPa in Fig. 1).

Altogether this implies a well-resolved Zn-Se percolation doublet (the above-mentioned weak plus strong TO modes) in ZnBeSe, instead of a singlet as earlier presumed. The

magnitude of splitting in the Zn-Se doublet ($\Delta \sim 30 \text{ cm}^{-1}$, refer to the inset in Fig. 1), almost as large as the Be-Se one, is, however, disconcerting.¹ For example in ZnBeTe the Zn-Te ($\Delta \sim 6 \text{ cm}^{-1}$) and Be-Te ($\Delta \sim 35 \text{ cm}^{-1}$) splittings scale in the ratio 1:6. For independent insight we performed *ab initio* calculations with the 2-imp. (Be) motif in ZnSe. The short Be-Se bonds create a local tension in ZnSe, giving rise to a local Zn-Se mode around Be ($\text{TO}_{\text{Zn-Se}}^{\text{Be}}$, weak—see the vibration pattern in Fig. 2) at a lower frequency than that of bulk ZnSe ($\text{TO}_{\text{Zn-Se}}^{\text{Zn}}$, strong). As expected, the *ab initio* splitting is small, of $\sim 8 \text{ cm}^{-1}$, corresponding to a position of the harmonic (uncoupled) weak $\text{TO}_{\text{Zn-Se}}^{\text{Be}}$ renormalized to the thick line in Fig. 2. We infer that the anharmonic coupling induces a massive frequency downshift of the weak $\text{TO}_{\text{Zn-Se}}^{\text{Be}}$ with respect to the *ab initio* prediction (by $\sim 22 \text{ cm}^{-1}$), the strong $\text{TO}_{\text{Zn-Se}}^{\text{Zn}}$ remaining unaffected. This suggests that the continua couple strongly to the weak TO and weakly to the strong one.

For a quantitative insight, we perform analysis of the TO line shapes using the formula $I(\omega) \sim [\alpha + \Gamma(\omega)]^2 [(\omega - \omega_0 - \Delta(\omega))^2 + (\alpha + \Gamma(\omega))^2]^{-1}$,¹³ where ω_0 is the frequency of the harmonic (uncoupled) TO mode, α accounts for all natural (not due to anharmonic coupling) contributions to its line-width (the original smoothly varying function versus ω in Ref. 13 is replaced by a constant), and $\Delta(\omega)$ and $\Gamma(\omega)$ are the real and imaginary parts of the phonon self-energy. These are expressed according to Eq. (5) in Shand *et al.*,¹³ that take into account an anharmonic fourth-order coupling V_4 (between pairs of phonons in the two-phonon continuum) on top of the anharmonic third-order one V_3 (between the TO mode and the two-phonon continuum). If $V_4=0$, $\Gamma(\omega)$ and $\Delta(\omega)$ relate separately to the two-phonon DOS, and to its Kramers-Krönig's transform, respectively.¹³ Otherwise ($V_4 \neq 0$), both quantities appear in the expressions of $\Gamma(\omega)$ and $\Delta(\omega)$. For simplicity the two-phonon DOS is designed as a semiellipse (which makes its Kramers-Krönig's transformation analytical¹⁴). The position, magnitude and spectral extension of the semiellipse are fixed by its upper end ω_c , and its semi-axes D and α , respectively.¹³ Generally, the effect of (a positive) V_4 is to distort the symmetrical V_3 -based $\Gamma(\omega)$ curve towards its high-frequency end (ω_c) (see, e.g., Fig. 3 in Ref. 13). To make it physically more meaningful, only one parameter is adjusted per TO mode, i.e., the strength $V_3^2 D$ of the cubic coupling, the criterion for validation being the ability to reproduce the TO-decoupling process (at $P \sim 7 \text{ GPa}$ for both TO modes). The other input parameters are determined as follows.

For the strong $\text{TO}_{\text{Zn-Se}}^{\text{Zn}}$ ω_0 is taken as the observed peak position, since anharmonic effects are presumably small, while for the weak $\text{TO}_{\text{Zn-Se}}^{\text{Be}}$ we use the *ab initio* value. As for the two-phonon DOS, the pressure dependence of the upper ends (ω_c) are derived by linear interpolations of the pressure dependencies of the decoupled 2TA (for $\text{TO}_{\text{Zn-Se}}^{\text{Be}}$) and LA+TA (for $\text{TO}_{\text{Zn-Se}}^{\text{Zn}}$) bands in pure ZnSe (refer to the dotted lines converging to $\sim 220 \text{ cm}^{-1}$ at 0 GPa in Fig. 2), after slight translations (by less than 2 cm^{-1}) needed to mimic alloying effects. The lower end, monitored by α once ω_c is known, provides an antiresonance on the low-frequency tail of the coupled TO (coupling regime) or uncoupled-two-phonon DOS (decoupling regime). The 2TA antiresonance is

clearly visible in our Raman spectra (refer to open squares in Fig. 1). For an insight into the (TA+LA)-related antiresonance we resort to the pure-TO Raman spectrum (14%Be, 0 GPa) available in Ref. 15 (top curve of Fig. 2). Clear antiresonances on each side of the strong TO therein, spaced by $\sim 15 \text{ cm}^{-1}$, correspond to $\alpha \sim 5 \text{ cm}^{-1}$, taken constant for all pressures. Last, the strength $V_4 D$ of the fourth-order coupling is constrained to the α value (within 5%), taken as $\sim 2.5 \text{ cm}^{-1}$ for all pressures.

As expected $V_3^2 D$ is larger for the weak $\text{TO}_{\text{Zn-Se}}^{\text{Be}}$ (with a value of $\sim 90 \text{ cm}^{-1}$) than for the strong $\text{TO}_{\text{Zn-Se}}^{\text{Zn}}$ ($\sim 10 \text{ cm}^{-1}$). The pressure-dependent line shapes of the weak TO (the strongly coupled one) over its decoupling process are shown in the inset of Fig. 2. The main features are well reproduced, i.e., the deepening of the antiresonance at $\sim 180 \text{ cm}^{-1}$ just when decoupling occurs (refer to open squares in Figs. 1 and 2; the arrow marks the frequency of the harmonic TO therein, for reference purpose), and the consequent appearance of the uncoupled 2TA band as an intense peak (refer to the star in Figs. 1 and 2) before it collapses into a damped feature away from the TO mode.

In brief, an anharmonic coupling greatly magnifies (by ~ 4) the natural splitting ($\Delta \sim 8 \text{ cm}^{-1}$) of the Zn-Se percolation doublet, giving a chance to observe its dependence on pressure. The two ZnSe-like TO branches are quasiparallel in Fig. 1 (spaced by $\sim 30 \text{ cm}^{-1}$, refer to the inset), indicating a constant Zn-Se splitting. *Ab initio* calculations at 0 and 10 GPa with the 2-imp. (Be) motif in ZnSe confirm the trend (not shown). We conclude that, as far as the Zn-Se bonds are concerned, the BeSe- and ZnSe-like regions of the crystal behave similarly under pressure.

B. Be-Se spectral range

This is not the case for the Be-Se bonds, as testified by singularity C in Fig. 1. We emphasize that C is not composition dependent, i.e., it occurs at the same critical pressure of $14 \pm 1 \text{ GPa}$ for all our samples, independently of the topology of the BeSe-like region. Apparently no effect is seen on whether the sample consists of a dispersion of finite-size clusters ($x < x_{\text{Be}}$), of the as-formed pseudoinfinite continuum (x just above x_{Be}) or of the dominant percolation cluster (x just above 0.5). This indicates a local origin at the bond scale. In fact, the ZC TO-DOS per Be atom obtained with the 2-imp. (Be) motif in ZnSe at 0 and 10 GPa do exhibit the C singularity. The curves are shown in the body of Fig. 3, specifying the vibration pattern per mode. In view of these, we identify the microscopic mechanism behind C as the transformation of $\text{TO}_{\text{Be-Se}}^{\text{Be}}$ (vibration along the Be-Se-Be chain, noted \parallel chain) from the bond-stretching type to the bond-bending type under pressure. The nature of the doubly degenerate $\text{TO}_{\text{Be-Se}}^{\text{Zn}}$ (vibrations perpendicular to the Be-Se-Be chain, noted \perp chain, in-plane and out-of-plane) remains unchanged, i.e., of the bond-bending type.

For more insight we performed similar *ab initio* calculations with the 2-imp. (Zn) motif in BeSe (Zn-dilute limit, not shown). The long Zn-Se bonds create a local compression in BeSe, leading to a local Be-Se mode close to Zn, i.e., $\text{TO}_{\text{Be-Se}}^{\text{Be}}$ (the vibration pattern is that shown in Fig. 2, where Zn and

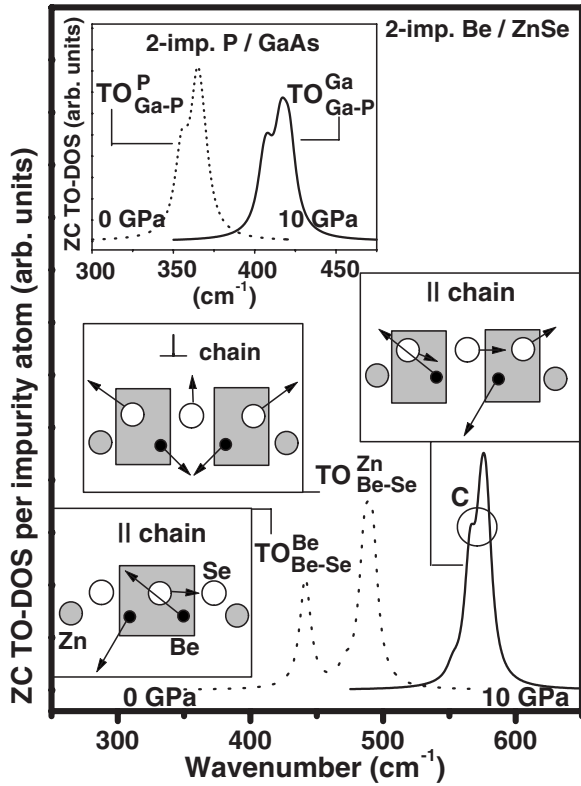


FIG. 3. *Ab initio* ZC TO-DOS per impurity of the 2-imp. Be (main curves) and P (inset) motifs in ZnSe- and GaAs-like supercells, respectively. The Be-Se vibration patterns are indicated, emphasizing the bond-stretching modes (dashed areas) in reference to feature C (circle).

Be are exchanged), at a higher frequency than the bulk BeSe mode, i.e., TO_{Be-Se}^{Be} . This gives a clear Be-Se percolation doublet, though the splitting is less than in the Be-dilute limit, of $\sim 11 \text{ cm}^{-1}$. Now, we observed the same splitting at 0 and 10 GPa, indicating that singularity C disappears when the Be-Se bonds are dominant in the alloy, thus not influenced by the Zn-Se bonds.

A further instructive case is that of GaAsP. Its short bond (Ga-P) exhibits a distinct percolation doublet ($\Delta \sim 12 \text{ cm}^{-1}$),¹ as in ZnBeSe, but, the parents (GaAs, GaP) adopt the same phase under pressure ($ZB \rightarrow Cmc$), and moreover at nearly the same critical pressure ($\sim 15 \pm 3 \text{ GPa}$). The ZC TO-DOS per P atom obtained at 0 and 10 GPa with the 2-imp. (P) motif in GaAs are shown in the inset of Fig. 3. The Ga-P percolation doublet is shifted upwards as a whole when approaching the phase transition, and no C-type convergence is observed. It emerges that the C singularity is not intrinsic to short bonds in alloys, but specific to the Be-Se bonds in ZnBeSe, when their fraction is

such (low or moderate) that they are forced to adopt the ZnSe-like RS phase under pressure.

For an intuitive discussion of the physics behind C we turn to the percolation model. Note that such phenomenological model relies on a scalar description of the alloy (linear-chain approximation) so that everything comes down to a question of bond-stretching forces only, by construction. Still, a parallel between the percolation model (mesoscopic scale) and *ab initio* calculations (microscopic scale) can be drawn by realizing that *bond-bending within a given impurity motif corresponds to bond stretching of the (like) surrounding bonds from the host matrix, and vice versa*. If we refer to the 2-imp. (Be) motif in ZnSe, this comes down to discuss the low- and high-frequency Be-Se modes in terms of Be-Se stretching within the BeSe- and ZnSe-like regions, respectively (see the shaded areas in the vibration patterns, Fig. 3), consistently with the terminology of the percolation model. Within such stretching-type model, the feature C can thus be understood as due to the progressive “freezing” of the Be-Se bonds from the minor BeSe-like region when this is forced to adopt the unnatural RS phase of the host ZnSe-like region. The oscillator strength is transferred to the close Be-Se bonds of the latter region.

IV. CONCLUSION

In brief, the percolation mesoscope reveals that the lattice dynamics of the ZnBeSe crystal basically changes when approaching the $ZB \rightarrow RS$ ZnSe-like transition under pressure, which is an unnatural transition for the Be-Se bonds. While the application of pressure reveals a percolation-type fine structure of the Zn-Se mode, that remains basically unaffected by pressure, the highly self-connected Be-Se bonds from the BeSe-like region “freeze” (the terminology is used within the scope of the percolation model), the oscillator strength being channeled to the less self-connected Be-Se bonds of the surrounding ZnSe-like region. This process, transparent for the Zn-Se dynamics, is completed ($\sim 14 \text{ GPa}$) before the actual transition to RS occurs ($\sim 23 \text{ GPa}$ at 24% Be). Generally this work shows how the percolation mesoscope may help to achieve further understanding of the pressure dependence of phonons in alloys beyond the usual VCA paradigm.

ACKNOWLEDGMENTS

This work has been supported by the Indo-French Center for the Promotion of Advanced Research (IFCPAR project No. 3204-1: Lattice dynamical and structural study of Be-based II-VI semiconductor alloys). The use of computer resources of PMMS at the University Paul Verlaine–Metz is greatly appreciated.

*Corresponding author; pages@univ-metz.fr

- ¹O. Pagès, J. Souhabi, A. V. Postnikov, and A. Chafi, *Phys. Rev. B* **80**, 035204 (2009).
- ²I. F. Chang and S. S. Mitra, *Adv. Phys.* **20**, 359 (1971).
- ³A. Mujica, A. Rubio, A. Muñoz, and R. J. Needs, *Rev. Mod. Phys.* **75**, 863 (2003).
- ⁴H. Luo, K. Ghandehari, R. G. Greene, A. L. Ruoff, S. S. Trail, and F. J. DiSalvo, *Phys. Rev. B* **52**, 7058 (1995).
- ⁵D. Stauffer, *Introduction to Percolation Theory* (Taylor & Francis, London, 1985).
- ⁶J. M. Soler, E. Artacho, J. D. Gale, A. García, J. Junquera, P. Ordejón, and D. Sánchez-Portal, *J. Phys.: Condens. Matter* **14**, 2745 (2002) <http://www.icmab.es/siesta/>.
- ⁷A. V. Postnikov, O. Pagès, and J. Hugel, *Phys. Rev. B* **71**, 115206 (2005).
- ⁸A. Polian, T. Ganguli, and S. K. Deb (private communication).
- ⁹W. C. Chou, C. M. Lin, R. S. Ro, C. S. Ho, D. Y. Hong, C. S. Yang, D. S. Chuu, T. J. Yang, J. Xu, and E. Huang, *Chin. J. Phys. (Taipei)* **35**, 266 (1997).
- ¹⁰C.-M. Lin, D.-S. Chuu, T.-J. Yang, W.-C. Chou, J.-A. Xu, and E. Huang, *Phys. Rev. B* **55**, 13641 (1997).
- ¹¹B. D. Rajput and D. A. Browne, *Phys. Rev. B* **53**, 9052 (1996).
- ¹²B. A. Weinstein, *Solid State Commun.* **24**, 595 (1977).
- ¹³M. L. Shand, H. D. Hochheimer, M. Krauzman, J. E. Potts, R. C. Hanson, and C. T. Walker, *Phys. Rev. B* **14**, 4637 (1976).
- ¹⁴P. Galtier, V. Lemos, M. Zigone, and G. Martinez, *Phys. Rev. B* **28**, 7334 (1983).
- ¹⁵O. Pagès, M. Ajjoun, J. P. Laurenti, D. Bormann, C. Chauvet, E. Tournié, and J. P. Faurie, *Appl. Phys. Lett.* **77**, 519 (2000).